

Time-Resolved Three-Dimensional Microscopy of Laser Photothermal Imaging Processes

Serguei G. Koulikov and Dana D. Dlott
Department of Chemistry
University of Illinois at Urbana-Champaign
600 S. Goodwin Ave., Urbana, Illinois

Abstract

Fundamental mechanisms of exposure by near-infrared (IR) laser pulses, of multilayer laser photothermal imaging media used as offset lithographic printing plates in computer-to-press or computer-to-plate applications, are investigated with time-resolved three-dimensional optical microscopy, with imaging pulses in the 1-ns to 10-μs range. Different behavior of different layers was observed depending on the pulse duration and pulse energy.

Introduction

In this paper we use three-dimensional time-resolved optical microscopy to investigate the dynamics of multilayer laser photothermal imaging materials. There has been great interest[1] in "computer-to-plate" or "computer-to-press" systems recently. Presstek, Inc. has developed the PEARL™ imaging platform[2]. PEARL is a patented, proprietary non-photographic, toxic-free, digital imaging and printing plate technology. Here we study a model imaging medium based on PEARL technology[2], which has a transparent substrate to let us look at the imaging material from the front and from the back. This medium consists of a polyester substrate, a thin (~20 nm) light absorbing titanium (Ti) interlayer, and a μm-thick imaging layer of oleophobic silicone polymer[3]. When the medium is exposed by near-IR pulses, the imaging layer is debonded. The imaged spot is cleaned and it becomes oleophilic. Exposing a series of spots in an imagewise manner produces a plate suitable for extended print runs (>100,000) with offset dry lithographic presses[2,3].

During the last few years these materials have been studied intensively in our laboratory[3-5]. The pulsewidth dependence of the exposure threshold was measured[4], as shown in Fig. 1. As the pulse duration is reduced, the exposure threshold decreases a great deal, by about a factor of thirty over the 1 ns to 30 μs range[4]. The smooth curve in Fig. 1 is a fit to a thermal conduction model discussed previously[4]. The pulsewidth dependence is understood qualitatively as follows. A threshold temperature $T_{th} \approx 600^{o}C$ must be reached to expose the imaging medium[3,4]. Near-IR light heats only the thin interlayer. The polymer is heated by thermal conduction. The volume of heated material increases with pulse duration, so exposure threshold increases with pulse duration as well. The threshold fluence curve levels off with very short pulses (< 10 ns) when the interlayer thickness becomes comparable to the diffusion length[4].

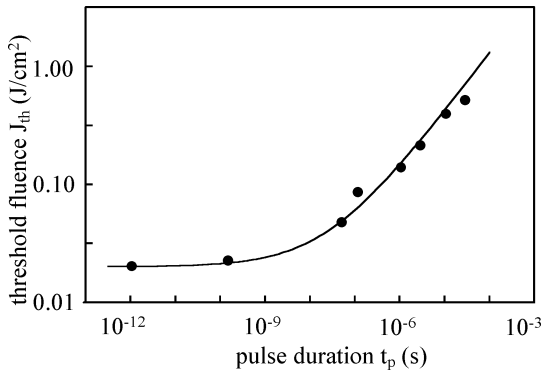

Figure 1. Pulse-width dependence of threshold fluence for media based on Presstek PEARL technology

Although the data in Fig. 1 are fit by a relatively simple model[4], we did not have a detailed picture of the exposure process for a complicated multilayer system. Such an understanding is believed necessary to improve existing media and to invent new media. To develop a better understanding of fundamental mechanisms, three-dimensional time-resolved optical microscopy experiments were performed with different duration pulses.

Experimental

Imaging Medium. The substrate was 175 μm thick transparent polyester (PET). The light-absorbing interlayer was ~20 nm thick sputtered Ti. The interlayer absorbs about 50% of incident light and it transmits about 20%[3]. The silicone imaging layer was about 2 μm thick[3].

Exposure Sources. Media were imaged with 1.064 μm wavelength near-IR pulses having a Gaussian radial profile. To produce pulses in the 1-ns to 30-μs range, two different lasers were used, as shown in Fig. 2. A continuously pumped Nd:YAG laser could be Q-switched to produce a 100-ns pulse, or externally pulse-sliced to produce pulses in the 1-30 μs range. A 1-ns pulse was generated by a Q-switched microlaser (Newport Inc., model NP-1030-10).

Ultrafast Microscopy. As shown in Fig. 2, a microscope (Olympus Corp., model BX60M) with a CCD camera (Sony Corp., model SSS-M254), a personal computer and digital frame grabber was used. For time-resolved microscopy, the illumination source was a <1-ns visible pulse from a dye laser pumped by a high-pressure nitrogen laser (Laser Photonics Corp., model LN203C). The frame grabber, imaging laser and illumination laser were triggered by a home-built pulse delay generator.

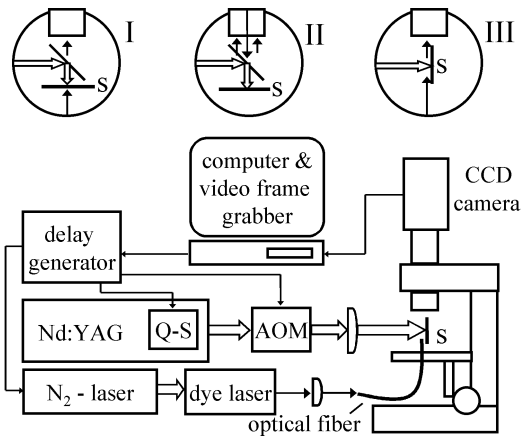

Figure 2. (Top) I, II, III denote different setups for transmission, reflection, and side-view imaging. S is the imaging sample. Double and single arrows indicate imaging pulses and illumination pulses, respectively. (Bottom) Block diagram of experimental apparatus for side-view imaging. AOM = acousto-optic modulator, Q-S = Q-switch.

The imaging medium was studied with three different setups, denoted I, II and III in Fig. 2. The imaging pulse was always incident on the silicone layer. Method I is a transmission measurement. The sample is placed on the microscope stage with silicone coating facing up. A visible illumination pulse is transmitted through the sample from the bottom of the microscope. To bring the imaging pulse to the silicone coating, a thin pellicle beamsplitter is used, which reflects near-IR and transmits visible light. Method II is a reflection measurement. The illumination pulse is brought to the sample through the microscope, from the top. Method III gives a side-view image. The sample is placed nearly vertically in the microscope, with a few degrees tilt, as shown in Fig. 2. The silicone layer faces out. The near-IR pulse comes from the side, normal to the silicone layer. The microscope is carefully focused onto the spot in the medium where the imaging pulse hits.

Keep in mind the ultrafast microscopy method gives only a single stroboscopic image with each shot. To reconstruct the time-dependent imaging process, a series of images is obtained at different times from fresh samples[3].

Results and Discussion

Two series of stroboscopic images of the dynamic exposure of an imaged spot, using 10-μs and 100-ns laser pulses, are shown in Figs. 3 and 4. The imaging laser beam radius r_0 =25 μm. Since exposure threshold is a function of duration, the best way to study directly comparable imaging processes is to use the exposure fluence which produces the *same size imaged area* for *both pulse durations*, which is near the point of maximum efficiency[5]. At the point of maximum efficiency, a Gaussian beam with radius r_0 produces a spot with radius r_s, $r_s^2=r_0^2/2$. The pulse energies were 13 μJ for the 10-μs pulses and 2.5 μJ for the 100-ns pulses. Notice the *energy* needed to image the same area with the shorter 100-ns duration pulses is five times less, but the *power* of the 100-ns pulses is about *twenty times as great* as the 10-μs pulses.

The leftmost columns of Figs. 3 and 4 are transmission images. These images mainly look at the metallic interlayer. The transmission of the interlayer is ~20%, so when the interlayer goes away, the transmitted light intensity increases by a factor of five. With 10-μs pulses, the interlayer comes off after ~10 μs. Careful examination of the images indicates the interlayer is partially melted in the middle of the imaged spot, where the Gaussian laser beam is most intense, but at the edge of the imaged spot the interlayer peels off almost intact in relatively large flaps. The driving force for peeling is thought to be gas from polymer decomposition and differential thermal expansion between interlayer and substrate. With 100-ns pulses, the interlayer behavior is much more violent, presumably due to the higher power of the 100-ns pulses. Tiny droplets of the interlayer material (Ti) are forcefully ejected from the medium by boiling or ablation. The ejected droplets can be seen off to the side in some of the images (e.g. 630 ns).

The center columns in Figs. 3 and 4 represent reflection images, which mainly see the silicone coating. With 10-μs pulses, the silicone develops a series of radial lines or wrinkles, which are attributed to differential thermal expansion. This column is quite similar to images shown in an earlier publication[3]. It is difficult to tell just what the silicone coating is doing from the reflection pictures alone.

The right columns in Figs. 3 and 4 represent side-view imaging. Now it can be seen that the silicone layer is forming a bubble in the silicone coating, which moves away from the imaged spot at high speed. The mechanism of bubble formation is believed to be expansion of hot gas formed by rapid thermal decomposition of silicone polymer near the silicone-Ti interface. The bubble is totally different with 10-μs and 100-ns pulses. The 10-μs bubble expands to a maximum radius of about 15 μm. The 100-ns bubble expands more violently to a maximum radius of about 50-μm before snapping back. The more violent expansion of the 100-ns bubble is attributed to the more powerful 100-ns pulses producing a higher temperature at the silicone-Ti interface in a shorter time.

When imaging materials are irradiated by 1-ns pulses, they behave much like the 100-ns case shown in Fig. 4, except about two times less energy is needed with the 1 ns pulse, and the power of the 1-ns pulse is about 50 times greater. To illustrate effects of the 1-ns pulse, Fig. 5 compares the silicone bubble when its size is maximum, produced by 10-μs, 100-ns and 1-ns pulses whose energies are adjusted to the point of maximum efficiency.

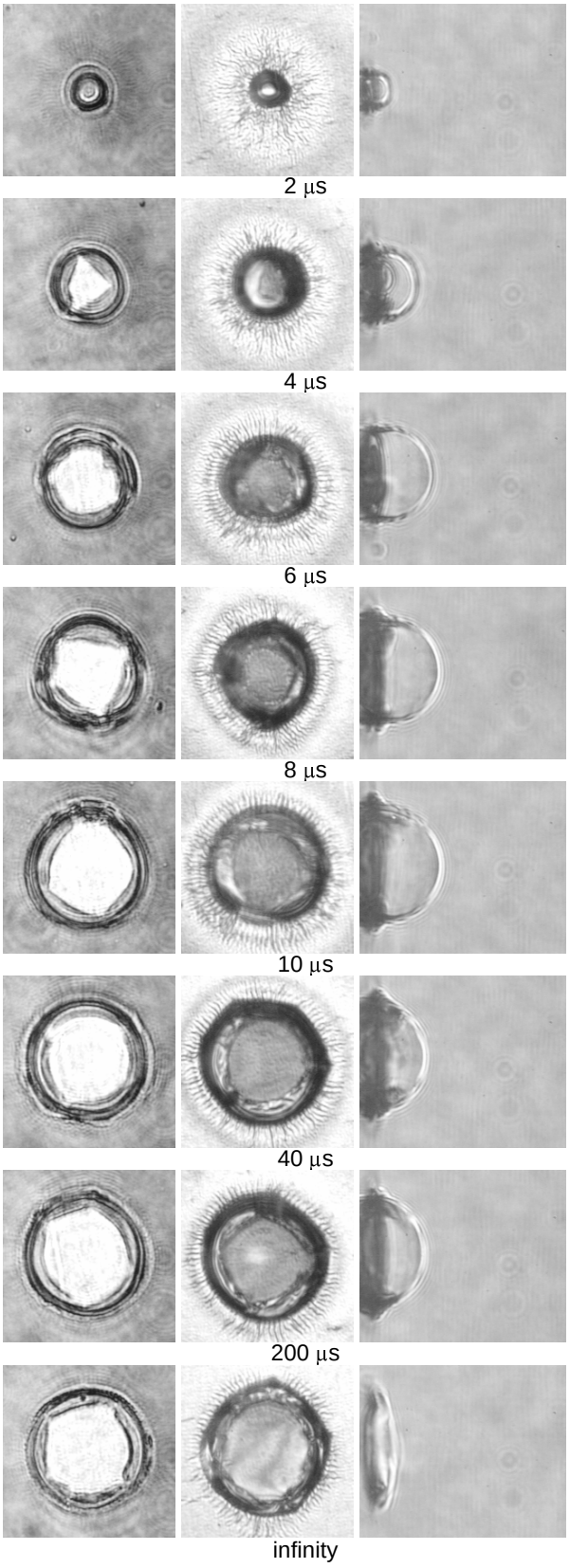

Figure 3. Transmission, reflection and side-view images taken at different delay times for a 10-μs imaging pulse. Image sizes: 54 x 54 μm, 54 x 65 μm

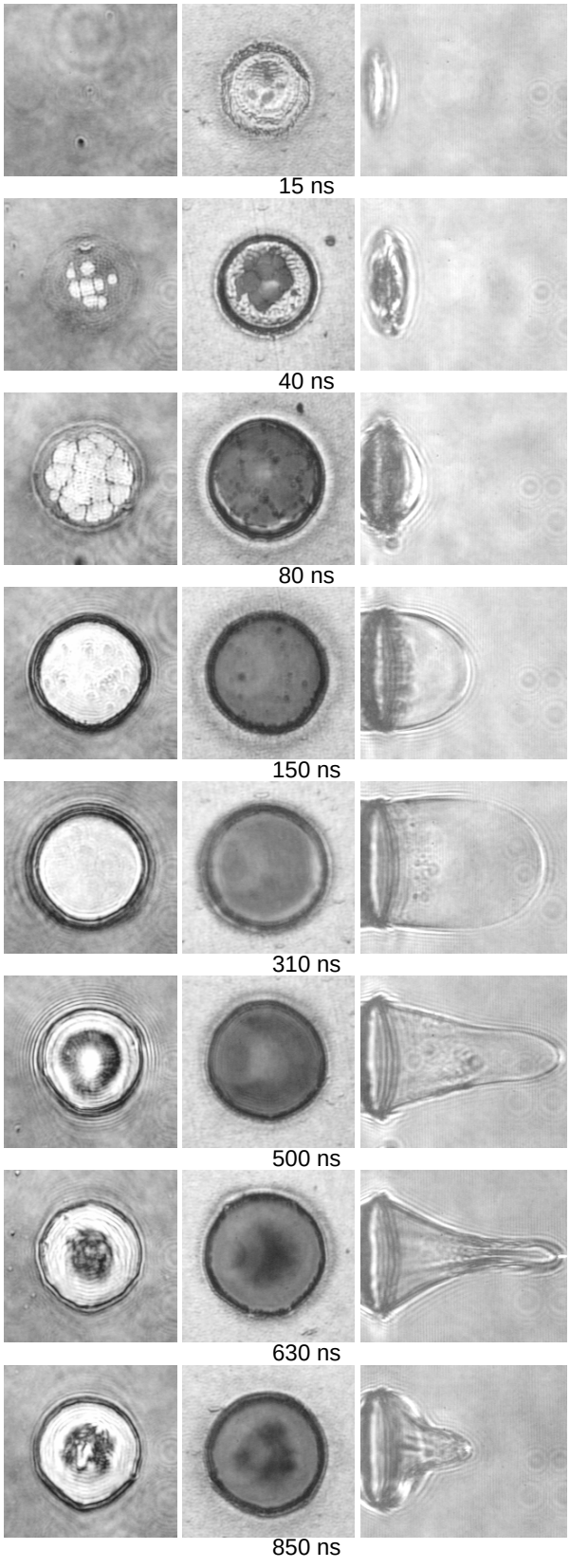

Figure 4. Transmission, reflection and side-view images taken at different delay time for a 100-ns imaging pulse. Image sizes: 54 x 54 μm, 54 x 65 μm

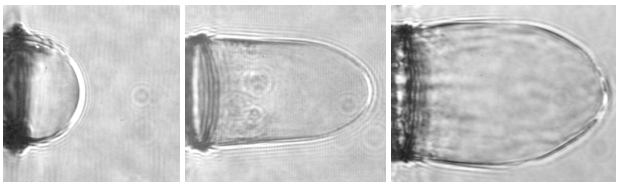

Figure 5. Side-view images of silicone bubble when the bubble is at its maximum size. From left to right: 10-μs pulse (13 μJ); 100-ns pulse (2.5 μJ) 1-ns pulse (1.2 μJ). Image height is 54 μm.

An interesting observation is that the static bubble sizes *after* the fast expansion and contraction phases are over are about the same independent of pulse duration, even though the pulse duration is varied over four orders of magnitude (1 ns to 10 μs). We interpret this to mean the amount of gas (decomposed polymer) produced and trapped in the bubble is about equal for all pulse durations. For the 1-ns pulse, the heated polymer volume is about 10 nm thick, determined by the thermal diffusion length[4]. With the 10-μs pulse, the heated polymer volume is about 1 μm thick, so the volume of heated polymer is vastly greater. Remarkably the volume of gas produced is about the same for all these pulse durations, so most of the gas must be formed right at the interfacial layer between the silicone and titanium, perhaps within about 10 nm of this interface.

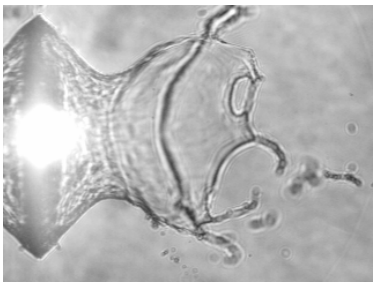

Figure 6. Bubble bursting during exposure at higher energy with a 100-ns pulse. Image size: 430 x *320 μm*

Another interesting observation occurs when the 100-ns pulse energy is increased to about sixty times the energy needed to expose an imaged spot. In this case the bubble expansion is so violent that the bubble bursts, as shown in Fig. 6 - a quite dramatic effect! The amount of energy needed to burst the bubble decreases a bit if the silicone layer is made thinner, but then the imaging medium cannot print as many copies.

Conclusion

Three-dimensional time-resolved optical microscopy provides unprecedented insights into the rather complicated mechanisms of laser photothermal imaging. It provides information about the time evolution of the different layers in the multilayer system during laser exposure. These studies should be useful in understanding how multilayer materials actually work, and how to optimize materials for different applications or to work with different writing engines.

Acknowledgment

This work was supported by a grant from Presstek, Inc. Additional support from the US Army Research Office, through contract No. DAAH04-96-1-0038, and from the National Science Foundation, grant No. DMR 94-04806 is gratefully acknowledged.

References

1. C. DeBoer, *J. Imaging. Sci. and Technol*., **42**, 63 (1998).
2. T. E. Lewis, M. T. Novak, K. T. Robichaud, and K. R. Cassidy, US patent #5,339,737, issued Aug. 23, 1994.
3. D. E. Hare, S. T. Rhea, D. D. Dlott, R. J. D'Amato, and T. E. Lewis, *J. Imaging. Sci. Technol*., **41**, 291 (1997).
4. D. E. Hare, S. T. Rhea, D. D. Dlott, R. J. D'Amato and T. E. Lewis, *J. Imaging. Sci. Technol*., **42**, 187 (1998).
5. D. E. Hare, S. T. Rhea, D. D. Dlott, *J. Imaging. Sci. Technol*., **41**, 588 (1997).

Biography

Serguei Koulikov received a M.S. in Physics from Moscow Institute of Physics and Technology in 1984 and a Ph.D. in Physics from the Institute of Spectroscopy at Troitsk, Russia in 1992. Dr. Koulikov joined the Institute of Spectroscopy in 1984, to research high-resolution molecular spectroscopy. From 1995 to 1997 he was a researcher at the University of California, Riverside, studying solid state spectroscopy. In 1997 he moved to the University of Illinois to research fundamental mechanisms of laser photothermal imaging.